Unoccupied electronic states in the band structure of NiAl(110)

G. R. Castro
Institut für Physikalische Chemie, Universität Bonn, Wegelerstrasse 12, D-5300 Bonn 1, Federal Republic of Germany

H. Dürr, R. Fischer, and Th. Fauster
Max-Planck-Institut für Plasmaphysik, EURATOM-Association, Boltzmannstrasse 2, D-8046 Garching, Federal Republic of Germany

(Received 6 November 1991)

The unoccupied electronic states of the clean NiAl(110) surface have been studied with angle-resolved inverse photoemission along the $\bar{\Gamma}\bar{X}$ and $\bar{\Gamma}\bar{Y}$ directions of the surface Brillouin zone. The use of a rotatable electron gun allows an independent variation of the incidence angle of the electrons and the exit angle of the photons. Measurements of the photon-emission characteristic of the dipole transitions observed in inverse photoemission can be used to determine the symmetry of the electronic states. For normal incidence of the electron beam, transitions along the ΓM line of the bulk Brillouin zone are detected and the results are compared to band-structure calculations available for the high-symmetry lines.

I. INTRODUCTION

In recent years there has been an increasing interest in studying alloy surfaces because the physical properties of these materials can differ significantly from those of the constituents and also vary with composition. One of the simplest metallic compounds is NiAl, which crystallizes in the CsCl structure. Its geometric and electronic properties have been investigated in a variety of studies.[1-4] Good agreement with band-structure calculations has been found for occupied electronic bulk states.[5] In contrast, very little is known about the unoccupied electronic levels. In this study we present measurements of the unoccupied electronic band structure of the NiAl(110) surface with angle-resolved inverse photoemission (IPE). In addition, information about the transition matrix elements has been obtained by detecting the photon-emission characteristic of the direct transitions.[6] The transition matrix elements for photoemission are generally believed to be determined by $\mathbf{A}\cdot\nabla V$, the scalar product of the vector potential $\mathbf{A}$ and the gradient of the potential, ∇V.[7] For dipole transitions the orientation of the dipole axis may be determined and conclusions for the symmetry of the final-state wave functions can be drawn. Section II describes briefly the experimental setup. In Sec. III the band-structure measurements and the angular dependence of the IPE data are presented and compared to the properties predicted by band-structure calculations. Section IV contains summary and conclusions of this study.

II. EXPERIMENT

The experiments were carried out in an UHV chamber with a base pressure below 1×10^{-10} Torr. The IPE experiments used a Geiger-Müller counter with iodine filling and a CaF_2 entrance window that performs as a bandpass detector for photons of 9.6 eV energy.[8] The electron gun with BaO cathode was mounted on a rotatable platform allowing a polarization analysis of the measured transitions.[6] The normal incidence of the electrons on the sample surface was determined by the dispersion of the IPE peaks and by total current spectroscopy.[9] The NiAl(110) sample was oriented 0.5° relative to the nominal [110] direction and mounted on a coolable three-axis manipulator.[10] The crystallographic orientation was determined *in situ* by impact-collision ion-scattering spectroscopy (ICISS).[11] The cleaning procedure for NiAl(110) has been described in detail in Ref. 12. The sample cleanliness was monitored by ion-scattering spectroscopy and the surface exhibited a well-ordered low-energy electron-diffraction pattern. The surface order was also checked with ICISS.

III. RESULTS AND DISCUSSION

A. Unoccupied band structure

In our IPE experiments we measure the dispersion of transitions between unoccupied electronic states which are separated by $\hbar\omega=9.6$ eV, the photon detection energy of our Geiger-Müller counter.[8] The results for the dispersions of the final-state energy versus wave-vector component $\mathbf{k}_{\parallel}$ parallel to the surface are shown in Fig. 1 for the two mirror planes of the NiAl(110) surface. The size of the data symbols indicates the intensity of the detected transitions. The data are obtained for different photon exit angles. Solid and open symbols indicate positive and negative incidence angles of the electrons. Both electron-incidence and photon-exit angles are measured clockwise relative to the sample normal. We can identify seven transitions $B1-B7$ in Fig. 1 which disperse with $\mathbf{k}_{\parallel}$. Near normal incidence the transitions $B2$ and $B3$ are observed from which the higher-lying one, $B3$, is clearly visible only in the $\bar{\Gamma}\bar{Y}$ azimuth which corresponds to the [001] crystal direction. It disperses downward in energy and seems to cross the slightly upwards-dispersing transition $B2$. For $\mathbf{k}_{\parallel}$ values larger than about 0.6 Å^{-1} both

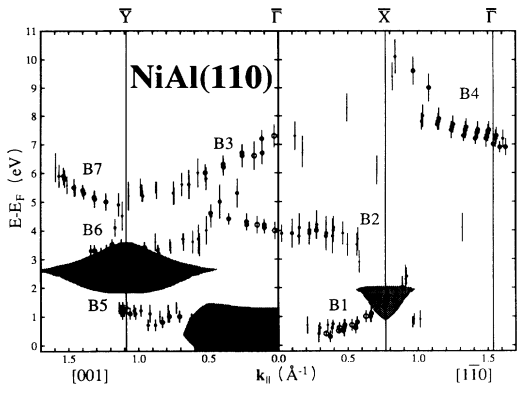

FIG. 1. Dispersions of the experimental final-state bands $B1-B7$ vs the wave-vector component $\mathbf{k}_{\parallel}$ parallel to the surface along the [001] and [1$\bar{1}$0] azimuths of NiAl(110). The shaded areas represent band gaps of the projected bulk band structure (Ref. 5). The size of the symbols indicates the intensity of the detected transitions. The data are obtained for different photon detection angles. Solid and open symbols are for electron incidence on the opposite and the same side as the photon detector relative to the surface normal, respectively.

peaks lose intensity and eventually emerge into the more intense transitions $B6$ and $B7$ near the $\bar{Y}$ zone boundary. Slightly above the Fermi level another structure, $B5$, is visible in this azimuth. In the $\bar{\Gamma}\,\bar{X}$ mirror plane the transition $B3$ can be seen only as a broad structure in the IPE spectra and is therefore not included in the $E(\mathbf{k}_{\parallel})$ diagram. In the second surface Brillouin zone a transition, $B4$, can be seen shifting downward in energy. At the $\bar{\Gamma}$ point the final-state energy of $B4$ is identical with $B3$ at normal incidence and we can speculate whether both transitions share the same final state. In Sec. III B we will present a polarization analysis of both transitions which indicates that $B3$ and $B4$ have different final states. Finally, a transition, $B1$, can be seen in the $\bar{\Gamma}\,\bar{X}$ azimuth dispersing from the Fermi level upwards to about 1.5 eV at the $\bar{X}$ surface Brillouin-zone boundary. The shaded area near $\bar{X}$ represents a band gap of the projected bulk-band structure. The band-structure calculation[5] in both mirror planes was available only for energy levels below 5 eV. Since near $\bar{X}$ the transition $B1$ lies within the band gap it can be assigned to a surface-induced resonance near $\bar{X}$. However, this interpretation depends crucially on the absolute position of the band gap near $\bar{X}$. Since $\mathbf{k}$-resolved photoemission experiments[5] show good agreement with theory, we can assume that the band gaps in the unoccupied states are reproduced reasonably well. In the $\bar{\Gamma}\,\bar{Y}$ mirror plane only projected band gaps for states with even parity exist for the energies shown in Fig. 1. These gaps are indicated as shaded areas in Fig. 1. We find that the transition $B6$ disperses through the upper part of the band gap centered at $\bar{Y}$ and should therefore consist only of odd final states. This must influence the emission characteristic of the transition and will be discussed in detail in Sec. III B.

Unfortunately, band-structure calculations in the two mirror planes[5] exist only for energies below about 5 eV. Along high-symmetry lines of the bulk Brillouin zone the band structure has been calculated up to about 11 eV above the Fermi level.[13,14] It is, therefore, not possible to describe theoretically all initial states of the transitions observed in IPE and to compare the measured dispersions directly to the theoretical band structure. At present this can unambiguously be done only for the Σ symmetry line along ΓM which is accessible on the (110) surface at normal electron incidence.[5] In this case the high-symmetry line coincides with the propagation direction of the electrons and we can immediately identify the initial-state band. If we describe the bands in a free-electron approximation the wave functions are plane waves with wave vectors $\mathbf{k}+\mathbf{g}$, where $\mathbf{g}$ is a reciprocal-lattice vector. The incident electrons can mainly couple to states inside the crystal propagating in the same direction, e.g., for normal incidence to states described by a reciprocal-lattice vector of the form $(2\pi/d)\,(-1,-1,0)$, where d is the lattice constant. Figure 2 shows a band-structure calculation along ΓM (solid lines).[13] The dispersion of the [$\bar{1}\,\bar{1}$0] free-electron band is indicated by the dotted line. In the band-structure calculation this initial state is described by a band with Σ_1 symmetry which shows hybridization with bands of equal symmetry above 10 eV and below 2 eV. The dotted line in Fig. 2 denotes the [$\bar{1}\,\bar{1}$0] nearly free-electron band shifted to lower energies by the photon energy of 9.6 eV. The crossings with the solid lines then characterize the points where direct transitions can be observed in IPE. From all five predicted transitions only the one at lowest final-state energy into a Σ_4 band can be described by the band-structure calculation. The initial state, however, would be near the top of the hybridization gap caused by the crossing of two Σ_1 states. The electrons in this state have a zero group velocity. That makes the coupling of the incident electrons to such an initial state very unlikely, and the

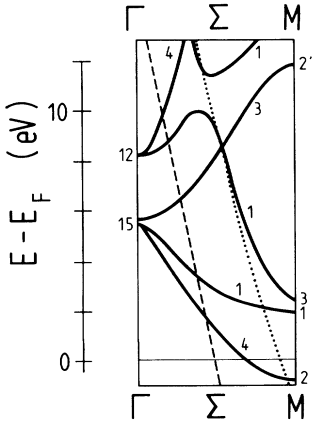

FIG. 2. Band-structure calculation (Ref. 13) of the unoccupied states of NiAl along the ΓM symmetry line. The dotted line shows the dispersion of the [$\bar{1}\,\bar{1}$0] free-electron band. The dashed curve shows the same band shifted down by the photon energy of 9.6 eV. At the intersections with the calculated bands direct transitions are possible.

transition therefore is not observed in the IPE spectra. We have to keep in mind that similar restrictions are possible for all other predicted transitions. With these limitations we could assign the peaks $B2$ and $B3$ in the IPE spectra to transitions into Σ_1 and Σ_3 final-state bands at energies of about 3.4 and 6.5 eV, respectively. The remaining two transitions cannot be observed in our spectra, probably due to the effects discussed above. To check our assignment of the peaks $B2$ and $B3$ is correct we determine the final-state symmetry from the measured photon emission characteristic. This will be done in Sec. III B.

B. Final-state symmetry

The intensity of the direct dipole transitions is described by $\mathbf{A}\cdot\langle f|\nabla V|i\rangle$, the scalar product of the vector potential $\mathbf{A}$ and the transition matrix element $\langle f|\nabla V|i\rangle$ between initial state $|i\rangle$ and final state $\langle f|$, where ∇V is the gradient of the potential. The orientation of the dipole axis is given by the matrix element and can be determined in IPE by measuring the angular distribution of the emitted radiation which was found to be in excellent agreement with the expected $\sin^2\Omega$ form, where Ω is the angle between dipole axis and detector.[6] If the dipole axis is known we can then determine the final-state symmetry.

Examples for transitions in the $\bar{\Gamma}\bar{X}$ mirror plane can be seen in Fig. 3, where a set of IPE spectra in this azimuth is shown. All spectra are normalized to equal height at 9 eV above the Fermi level. Let us focus first on the two spectra taken near normal electron incidence in the top part of Fig. 3. The spectra are taken with the detector placed along the $\bar{\Gamma}\bar{X}$ and the $\bar{\Gamma}\bar{Y}$ direction with a photon takeoff angle of 60° relative to the sample normal. Both peaks $B2$ and $B3$ are clearly discernible in the $\bar{\Gamma}\bar{Y}$ spectrum but only peak $B2$ is seen with the detector placed along $\bar{\Gamma}\bar{X}$. In this spectrum a broad structure is seen instead of peak $B3$. For symmetry reasons at normal electron incidence the dipole axis can either be oriented normal to the sample surface or parallel to it. In the first case we do not expect any intensity variations by changing the azimuthal position of the detector while keeping the exit angle to the sample normal fixed. This is seen for peak $B2$ and we can conclude that the dipole axis for this transition is oriented normal to the surface. In the preceding section the final state of $B2$ was identified as the $[\bar{1}\,\bar{1}0]$ free-electron state, which is totally symmetric (Σ_1). Since the vector ∇V points along the sample normal and is therefore of even parity relative to both mirror planes, i.e., totally symmetric, the final state also must be of Σ_1 symmetry to assure a nonvanishing matrix element. This Σ_1 final-state symmetry is in agreement with the band-structure calculation[13] in Fig. 2. The transition $B3$ shows intensity variations for an azimuthal rotation of the sample in contrast to $B2$. This can be explained by a dipole axis lying parallel to the surface. With similar arguments as for $B2$ we can then deduce a Σ_4 symmetry for the final state, i.e., it has even parity relative to $\bar{\Gamma}\bar{X}$ and odd parity relative to $\bar{\Gamma}\bar{Y}$ (Ref. 5). This, however, is in contrast to the band-structure calculation,[13] which predicts a Σ_3 band. In order to decide whether this discrepancy is due to some initial-state umklapp process or a failure of the theory, more band-structure calculations are needed, especially to test the dispersion of $B3$ along $\bar{\Gamma}\bar{Y}$.

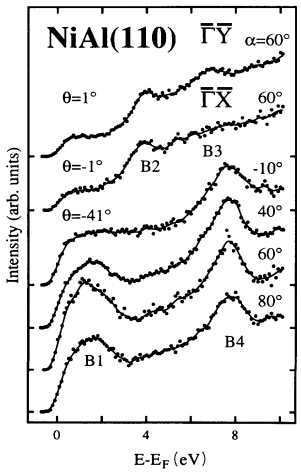

FIG. 3. Angle-resolved inverse-photoemission spectra near the $\bar{\Gamma}$ point of the reduced surface Brillouin zone for various photon detection angles.

The lower part of Fig. 3 contains a series of IPE spectra for different photon-detection angles at an electron incidence angle of $\theta=-41°$. The transition $B1$ at a final-state energy of about 1.7 eV shows strong polarization effects and has completely vanished at a detection angle of $\alpha=-10°$. At this position the detector points along the dipole axis. This shows that the dipole axis lies in the $\bar{\Gamma}\bar{X}$ mirror plane and that the final state has even parity relative to the $\bar{\Gamma}\bar{X}$ mirror plane. The transition $B4$ at a final-state energy of 8 eV shows no intensity variation with the detection angle which can be explained by a dipole axis normal to the $\bar{\Gamma}\bar{X}$ mirror plane and, therefore, an odd final state. It is interesting to note that this transition $B4$ has at the surface Brillouin-zone boundary $\bar{\Gamma}$ the same energy as the transition $B3$ at $\bar{\Gamma}$. At this final-state energy the band-structure of Fig. 2 shows only a Σ_1 and a Σ_3 band with even and odd parity relative to $\bar{\Gamma}\bar{X}$, respectively. The initial state of $B4$ is unknown, but we know that it must have an even parity relative to $\bar{\Gamma}\bar{X}$ in order to produce a nonzero overlap with the even plane wave of the incoming electrons. With the observed dipole orientation it immediately follows that the final state of $B4$ is of Σ_3 symmetry in agreement with the band-structure calculation in Fig. 2. This shows that in spite of the coincidence in energy of the transitions $B3$ and $B4$ at $\bar{\Gamma}$, these transitions do not share the same final state.

Also, the transitions $B5$–$B7$ detected in the $\bar{\Gamma}\bar{Y}$ direction exhibit clear polarization effects which allow a determination of the final-state symmetries. A set of IPE spectra at an angle of incidence of $\theta=64°$ for four different detection angles is shown in Fig. 4. The three observed transitions are located in the surface Brillouin zone near the $\bar{Y}$ point. As mentioned in Sec. III A the transition $B6$ disperses along the edge of a band gap in the even final states and should therefore consist near $\bar{Y}$ mainly of odd

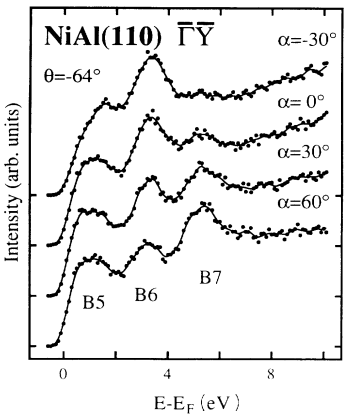

FIG. 4. Angle-resolved inverse-photoemission spectra at an electron incidence angle of $-64°$ in the $\bar{\Gamma}\,\bar{Y}$ mirror plane for various photon detection angles.

final-state wave functions. The intensity of peak $B6$ in Fig. 4 shows, however, a clear dependence with the photon-detection angle. That indicates that the final states of $B6$ consist instead of a mixture of odd and even states, which is not too surprising, since the energy position is very close to the band-gap edge. The transition $B7$ in Fig. 4 seems to have merely final states with even parity relative to $\bar{\Gamma}\,\bar{Y}$. At a photon detection angle of roughly $\alpha = -30°$ it has almost vanished and we can conclude that the dipole axis is oriented about 30° away from the surface normal. The energy position of peak $B5$ seems to shift with the detection angle which may be due to two different transitions with almost identical energy positions but with different emission characteristics.

IV. SUMMARY AND CONCLUSIONS

We have measured the dispersion of direct transitions on NiAl(110) with IPE in the $\bar{\Gamma}\,\bar{X}$ and $\bar{\Gamma}\,\bar{Y}$ mirror planes. From the angle-resolved IPE spectra seven transitions could be identified. By measuring the photon-emission characteristic the final-state symmetry could be determined. The transitions $B2$ and $B4$ at $\bar{\Gamma}$ were identified in a band-structure calculation along the ΓM symmetry line and good agreement in final-state energy and symmetry was found. The determined symmetry of the other transitions will serve as a further identification test in future band-structure calculations.

ACKNOWLEDGMENTS

We acknowledge stimulating discussions and support by V. Dose. G.R.C. enjoyed the hospitality of the Max Planck Institute for Plasma Physics.

[1]G. R. Castro, H. Isern, U. Schneider, M. Stöcker, and K. Wandelt, Vacuum **41**, 393 (1990).
[2]S. P. Chen, A. F. Voter, and S. J. Srolovitz, Phys. Rev. Lett. **57**, 1308 (1986).
[3]H. L. Davis and J. R. Noonan, Phys. Rev. Lett. **54**, 566 (1985).
[4]D. R. Mullins and S. H. Overbury, Surf. Sci. **199**, 141 (1988).
[5]S.-C. Lui, J. W. Davenport, E. W. Plummer, D. M. Zehner, and G. W. Fernando, Phys. Rev. B **42**, 1582 (1990).
[6]Th. Fauster, R. Schneider, and H. Dürr, Phys. Rev. B **40**, 7981 (1989).
[7]N. V. Smith, Rep. Prog. Phys. **51**, 1227 (1988), and references therein.
[8]V. Dose, Appl. Phys. **14**, 117 (1977).
[9]R. Schneider, H. Dürr, Th. Fauster, and V. Dose, J. Vac. Sci. Technol. A **8**, 3363 (1990).
[10]H. Dürr, Th. Fauster, and R. Schneider, J. Vac. Sci. Technol. A **8**, 145 (1990).
[11]Th. Fauster, Vacuum **38**, 179 (1988).
[12]H. Isern and G. R. Castro, Surf. Sci. **211/212**, 865 (1989).
[13]J. W. D. Connolly and K. H. Johnson, in *Electronic Density of States*, Natl. Bur. Stand. (U.S.) Spec. Publ. No. 323, edited by L. H. Bennett (U.S. GPO, Washington, D.C., 1979), p. 19.
[14]K. Pechter, P. Raste, A. Neckel, R. Eibler, and K. Schwarz, Monatsh. Chem. **112**, 317 (1981).

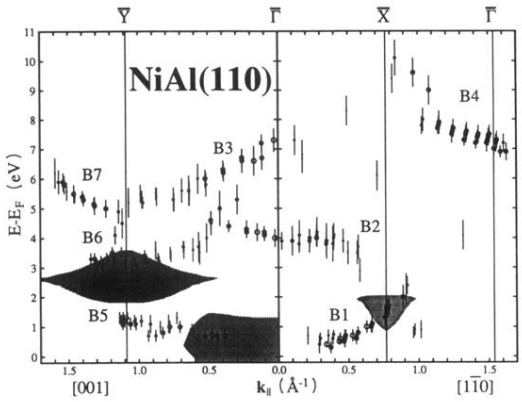

FIG. 1. Dispersions of the experimental final-state bands $B1-B7$ vs the wave-vector component $\mathbf{k}_{\|}$ parallel to the surface along the [001] and [1$\bar{1}$0] azimuths of NiAl(110). The shaded areas represent band gaps of the projected bulk band structure (Ref. 5). The size of the symbols indicates the intensity of the detected transitions. The data are obtained for different photon detection angles. Solid and open symbols are for electron incidence on the opposite and the same side as the photon detector relative to the surface normal, respectively.